

DOI:10.13476/j.cnki.nsbtdqk.2020.0054

张建梅,马燮铤,李艳忠.1980—2016年黄河中游河龙区间植被动态及其对径流的影响[J].南水北调与水利科技(中英文),2020,18(3):91-109. ZHANG J M, MA X Y, LI Y Z. Vegetation dynamics and its impact on runoff in the Hekouzhen-Longmen region of the middle reaches in the Yellow River from 1980-2016[J]. South-to-North Water Transfers and Water Science & Technology, 2020, 18(3): 91-109. (in Chinese)

1980—2016年黄河中游河龙区间植被动态及其对径流的影响

张建梅¹, 马燮铤², 李艳忠²

(1. 南京信息工程大学 大气科学学院, 南京 210044; 2. 南京信息工程大学 水文与水资源工程学院, 南京 210044)

摘要:黄河中游河龙区间是我国退耕还林/还草工程(grain for green project, GGP)实施的重点区和典型区, 定量评估该流域植被动态及其对径流的影响, 对流域水资源可持续利用以及 GGP 工程的生态水文效应评价具有重要意义。该研究基于遥感、GIS 技术、数理统计和布迪克弹性系数法, 利用 7 期植被类型数据, 定量评估了 37 年来河龙区间植被覆盖的时空变化格局及其对径流变化的影响。结果表明: 植被变化并未显著地改变河龙区间各植被类型的时空分布格局; GGP 的实施改变了各植被类型的平衡状态和转化速度; 植被变化是 GGP 实施后 10 年(2000—2010 年)径流下降的主要驱动因素, 但随后降水的持续增加, 使得植被的“减水效应”趋于缓和。

关键词:黄河中游; 河龙区间; 植被变化; 退耕还林/还草工程; 贡献率

中图分类号: P333 文献标志码: A 开放科学(资源服务)标志码(OSID):



植被变化作为土地利用/覆被变化(LUCC)主要形式之一, 可影响水分和能量的再分配。近些年, 区域乃至全球尺度的植被变化已被广泛关注和报道^[1-2], 特别是剧烈的人类活动所引起的植被变化对陆地水资源分布格局、水循环过程及碳循环均产生了较为深远的影响^[3-4]。我国政府为了实现“再造一个山川秀美的西北地区”的目标, 实施了多项植被恢复工程, 其中 1999 年实施的退耕还林/还草工程(grain for green project, GGP)是发展中国家实施的最大的植被恢复工程。该工程的实施将会对区域乃至全国尺度的植被变化、资源环境的可持续利用产生直接影响^[5]。因此, 定量评估 GGP 实施对植被变化的格局、动态趋势的影响, 以及植被变化对径流变化的影响, 将有助于深入理解植被的生态水文效应并制定生态恢复措施。

黄河中游处于我国半干旱半湿润过渡带, 水土流失、洪水灾害和水环境恶化较为严重, 是植被恢复工程的重点区域。诸多学者对黄河中游植被变化进行了研究, 如梁伟等^[6]利用 1975、1986 和 1997 年 3 期遥感影像分析了黄河中游多沙粗沙区土地利用变化, 发现耕地、林地、草地是 GGP 实施前土地利用变化的主导类型; 李滚等^[7]利用 1977、1997 和 2006 年 3 期土地利用数据, 发现耕地、草地、林地和未利用地的变化速度及其转移率变化受退耕还林(草)政策影响很大, 其中林地面积持续增加, 耕地、未利用地减少, 草地先减后增; 周德成等^[8]利用 1978—2010 年 6 期 LUCC 数据研究了 GGP 对河龙区间安塞县各地类的影响, 发现 GGP 使研究区整体处于不平衡态势, 耕地先增后减, 林地先减后增, 灌木林地和草地减少; 刘昌明等^[9]发现 2000 年来黄河中游

收稿日期: 2019-09-19 修回日期: 2019-10-30 网络出版时间: 2019-11-25
网络出版地址: <http://kns.cnki.net/kcms/detail/13.1334.TV.20191125.1148.002.html>
基金项目: 国家自然科学基金项目(41877158; 41701019)
作者简介: 张建梅(1995—), 女, 江苏南通人, 主要从事区域气候变化与水文水资源方向研究。E-mail: 18252088753@163.com
通信作者: 马燮铤(1963—), 男, 浙江宁波人, 教授, 博士, 主要从事气候变化与水文水资源方向研究。E-mail: xyma@nuist.edu.cn

11 个子流域的叶面积指数(LAI)、归一化植被指数(NDVI)均呈增大趋势,以河龙区间变化最为显著。然而,对于黄河中游,尤其是植被变化显著的河龙区间,2000—2015 年植被的格局与趋势的定量分析相对薄弱。对于黄河中游植被变化对径流的影响,学者们也开展了大量研究工作,如刘昌明和钟骏襄^[10]发现黄河中游森林的增加会减少年径流量,减少洪水流量,增加地下水径流量,从而改变径流分配的过程;Cao 等^[11]认为大规模的造林活动可能加剧半干旱半湿润区的水资源短缺,最终导致造林成活率和植被覆盖度降低;Chen 等^[12]认为黄土高原地区植被如果再持续恢复将减少水资源可利用量。但针对植被恢复工程实施重点区域—河龙区间—的植被水文效应,特别是 2010 年后,其植被变化对径流的影响研究较少。

基于此,本文选择植被变化显著的河龙区间作为研究区,并利用 7 期土地利用数据(1980 年代末至 2015 年)及降水、径流等水文气象数据,进行了植被空间分布格局动态分析、植被变化的定量评估及植被变化对径流的贡献分析,旨在揭示植被在研究区内的时空分布特征,定量评估 GGP 对河龙区间植被变化的方向、速度和趋势的影响,阐明植被变化对径流的影响,以期理解黄河中游河龙区间植被动态变化过程,为客观评估 GGP 的效果提供参考。

1 研究区和方法

1.1 研究区概况

本研究区位于黄河河龙区间,即河口镇至龙门区间,集水面积 11.2 万 km²,约占黄河总流域面积的 14.8%。该区间处于我国半干旱半湿润过渡带,属温带大陆性季风气候,降水从东南向西北递减,空间分布差异显著且季节分配不均匀,主要集中在 6—9 月,使河龙区间成为黄河流域水土流失最为严重的地区^[13-14]。区间多年平均降雨量约为 451.7 mm,蒸发皿测得的蒸发量约为 1 500 mm^[15]。丘陵广布,地势北高南低,东西高,中间低,海拔大都在 1 000~1 500 m。

1.2 数据源

本文采用的 7 期植被类型数据(1980 年代末、1990、1995、2000、2005、2010、2015 年)来自中国科学地理科学与资源研究所数据共享中心(<http://www.resdc.cn/>),空间分辨率为 1 km。根据研究区植被的特征及景观变化差异,参照《土地利用现状调

查技术规范》,对研究区土地利用类型进行重新合并处理,将土地利用类型分为 9 类,耕地、有林地、灌木地、疏林地、其他林地、高覆盖度草地、中覆盖度草地、低覆盖度草地和其他用地。

降水、温度和风速等气象数据来自中国气象局国家气象信息中心(<http://data.cma.cn/>),时间为 1980—2016 年。1980—1997 年的年径流量数据来自国家水文年鉴整编的月径流量数据,1998—2016 年的年径流量数据来自黄河水资源公报(<http://www.yellowriver.gov.cn/other/hhgb/>)。为了消除人类活动取用水(农田灌溉、工业、居民生活、城镇公共等)对径流量的影响,本文所用径流量为忽略人类活动影响的还原径流量^[16-17]。

1.3 研究方法

1.3.1 植被变化量化模型

运用 ArcGIS 10.2 及 ENVI 5.3 的空间分析模块,对 7 期植被类型进行统计和叠加分析,在各植被类型面积转移矩阵的基础上计算动态变化度,分析河龙区间近 35 年来的植被覆盖变化规律。模型中涉及到的主要指标如下^[8,15]:

N_c 、 T_c 、 P_s 和 R_s 分别为单一植被类型的面积净变化、总变化、趋势与状态指数和净变化速度。

$$N_c = \frac{U_b - U_a}{U_a} \times 100\% = \frac{\Delta U_{in} - \Delta U_{out}}{U_a} \times 100\% \quad (1)$$

$$T_c = \frac{\Delta U_{in} + \Delta U_{out}}{U_a} \times 100\% \quad (2)$$

$$P_s = \frac{N_c}{T_c} = \frac{\Delta U_{in} - \Delta U_{out}}{\Delta U_{in} + \Delta U_{out}} \quad (3)$$

$$R_s = \left(\sqrt[T]{\frac{U_b}{U_a}} - 1 \right) \times 100\% = \left[\sqrt[T]{\frac{U_a + (\Delta U_{in} - \Delta U_{out})}{U_a}} - 1 \right] \times 100\% \quad (4)$$

S_a 、 S_s 、 P_t 和 R_t 分别为总体植被的面积净变化、总变化、趋势与状态指数和净变化速度。

$$S_a = \frac{\sum_{i=1}^n |U_{bi} - U_{ai}|}{2 \sum_{i=1}^n U_{ai}} \times 100\% = \frac{\sum_{i=1}^n |U_{in-i} - U_{out-i}|}{2 \sum_{i=1}^n U_{ai}} \times 100\% \quad (5)$$

$$S_s = \frac{\sum_{i=1}^n |U_{in-i} + U_{out-i}|}{2 \sum_{i=1}^n U_{ai}} \times 100\% = \frac{\sum_{i=1}^n \Delta U_{out-i}}{\sum_{i=1}^n U_{ai}} \times 100\% = \frac{\sum_{i=1}^n \Delta U_{in-i}}{\sum_{i=1}^n U_{ai}} \times 100\% \quad (6)$$

$$P_t = \frac{S_a}{S_s} = \frac{\sum_{i=1}^n |U_{out-i} - U_{in-i}|}{\sum_{i=1}^n |U_{out-i} + U_{in-i}|}, 0 \leq \frac{S_a}{S_s} \leq 1 \text{ 且}$$

$$0 \leq P_t \leq 1, S_s \neq 0 \quad (7)$$

$$R_t = \left[\frac{\sum_{i=1}^n U_{ai} + \frac{1}{2} \sum_{i=1}^n |U_{bi} - U_{ai}|}{\sum_{i=1}^n U_{ai}} - 1 \right] \times 100\% =$$

$$\left[\frac{\sum_{i=1}^n U_{ai} + \frac{1}{2} \sum_{i=1}^n |U_{in-i} - U_{out-i}|}{\sum_{i=1}^n U_{ai}} - 1 \right] \times 100\% \quad (8)$$

式中： U_a 、 U_b 分别为研究初期和末期某一植被类型的面积； U_{out} 为研究时段内某一植被类型转变为其他植被类型的面积之和； U_{in} 为同时期其他植被类型转变为该植被类型的面积之和； U_{ai} 、 U_{bi} 分别为研究初期和末期第 i 种植被类型的面积； U_{out-i} 为研究时段内第 i 种植被类型转变为其他植被类型的面积之和； U_{in-i} 为其他植被类型转变为第 i 种类型的面积之和； n 为植被类型总数； T 为研究时段。

1.3.2 突变点检测和潜在蒸散发计算

利用非参数 Mann-Kendall 法对径流序列的突变点进行检测,该方法是非参数统计常用的一种检验方法,能够检验线性或非线性趋势,常被用于水文气象要素序列的变化分析^[18]。

潜在蒸散量采用参考作物蒸散发计算方法^[19]获取,公式为

$$ET_0 = \frac{0.408\Delta(R_n - G) + \gamma \frac{900}{T_a + 273} u_2 \cdot VPD}{\Delta + \gamma(1 + 0.34u_2)} \quad (9)$$

式中： ET_0 为日潜在蒸散发,mm/d； Δ 为温度-饱和水汽压曲线斜率, kPa/°C； R_n 为地表净辐射, MJ/(m²·d)； G 为土壤热通量, MJ/(m²·d)； γ 为干湿球常数, kPa/°C； T_a 为 2 m 高度平均日气温, °C； u_2 为 2 m 高度风速, m/s, VPD 为水汽压差, kPa。

1.3.3 植被对径流影响量化模型

弹性系数定义为因变量的变化率与自变量的变化率的比值,常被作为一个变量对另一个变量的敏感性指标^[20-21]。径流量对其他因素的弹性可以表达为

$$E_x = \lim_{\Delta x/x} \left[\frac{\Delta R/R}{\Delta x/x} \right] = \frac{\partial R}{\partial x} \times \frac{x}{R} \quad (10)$$

式中： E_x 为弹性系数； R 为径流量； x 为特定的因

素,如降水、潜在蒸散发等。

对于一个闭合流域而言,实际蒸散发 ET_a 可以通过水量平衡方程进行估算,

$$ET_a = P - Q - \Delta S \quad (11)$$

式中： ET_a 为实际蒸散发,mm； P 为降水量,mm； ΔS 为土壤水储量变化,mm。较长时间尺度(5 年以上)而言,其土壤水储量变化认为不变(即 $\Delta S \approx 0$)，公式(11)可简化为

$$ET_a = P - Q \quad (12)$$

长时间尺度实际蒸散发 ET_a 可以通过布迪克理论方法估算,该方法已作为评估气候和下垫面变化相互联系和反馈的有效手段^[22,23]。其中较为广泛使用的模型为 Choudhury-Yang^[23-25]：

$$ET_a = \frac{P \cdot ET_0}{(P^n + ET_0^n)^{1/n}} \quad (13)$$

式中： P 为降水量； n 为反映流域下垫面特征参数,比如地形,地貌,土壤和植被等,研究发现,当地形等因素变化不大时,参数 n 和植被变化密切相关^[26],并可以通过植被指数进行估算。径流变化可以看作降水、潜在蒸散发和下垫面参数 n 的全微分,而植被对径流变化的贡献量(Cr_n)可以表达为

$$Cr_n = \epsilon_n \frac{\Delta n}{n} R \quad (14)$$

$$\epsilon_n = \frac{\ln(1 + \varphi^n) + \varphi^n \ln(1 + \varphi^{-n})}{n[(1 + \varphi^n) - (1 + \varphi^n)^{1/n+1}]} \quad (15)$$

式中： ϵ_n 为径流对下垫面参数 n 的弹性系数； $\varphi = ET_0/P$ 。

2 研究结果

2.1 植被空间分布格局动态

图 1 展示了河龙区间 1980—2015 年 7 个时段的植被空间分布,图 2 列出了各植被类型面积比例的统计信息。由图 1 可知,研究区内不同时期各植被类型并未表现出显著的空间差异性。由图 2 统计信息可知,整个研究区各时期面积最大的植被类型均为耕地(变化范围为 31.0%~32.3%),其次为低覆盖度草地(19.4%~21.8%)、中覆盖度草地(18.9%~23.8%)、灌木林(7.5%~8.1%)、高覆盖度草地(3.4%~3.8%)和疏林地(2.8%~3.3%)。占地面积最小的植被类型为有林地和其他林地(变化范围为 2.3%~3.7%)。由此可知,GGP 并未显著地改变各植被类型的空间分布格局。

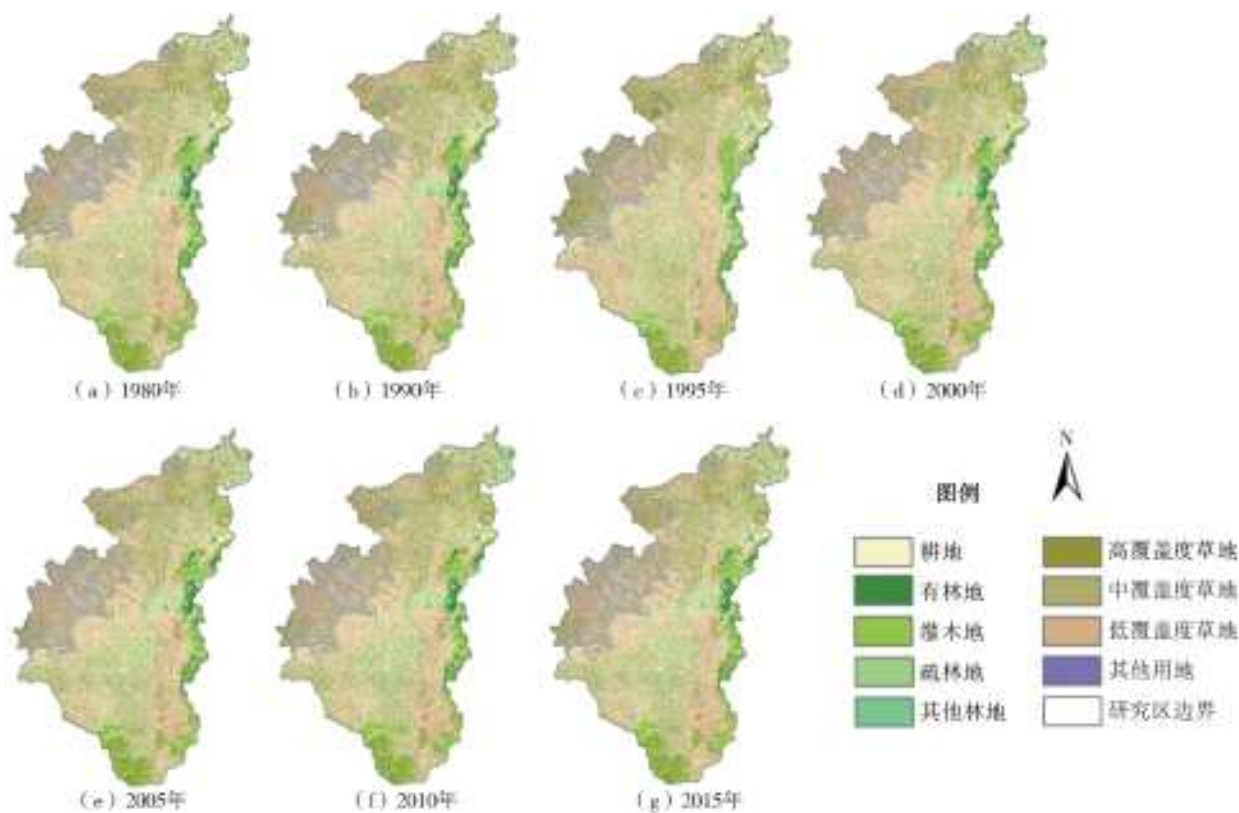


图 1 黄河中游河龙区间 1980—2015 年 LUCC 空间分布

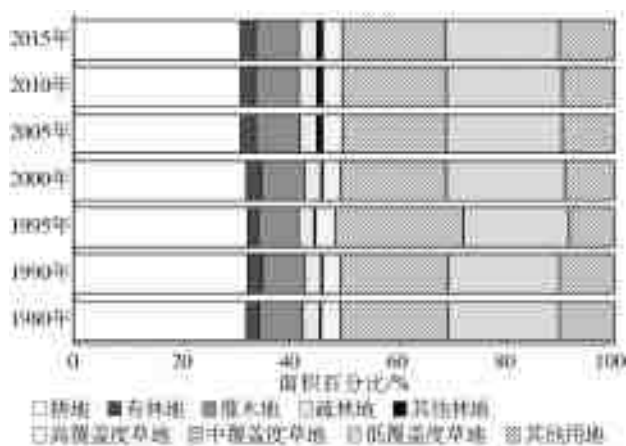


图 2 黄河中游河龙区间各植被类型面积比例

2.2 植被变化的定量评估

GGP 的实施改变了流域各植被类型的变化速度和平衡状态。由表 1, GGP 实施前的三个阶段 (1980—1990、1990—1995 和 1995—2000 年), 各植被类型的趋势状态指数 P_i 均较小, 说明各植被类型均处于动态平衡状态。耕地、林地、草地的总变化量较大 (T_c 基本大于 100%), 而数量并未发生大的变化, 说明这三种植被类型在空间转换上比较剧烈, 主要可能由于不断大规模开垦林地、草地为农田, 随着耕种年限增加土壤肥力下降后弃耕^[15]。

GGP 实施后的三个时期 (2000—2005、2005—2010 和 2010—2015 年), 2000—2010 年各植被类型

的趋势状态指数 P_i 的绝对值增大, 说明各植被类型以单向转换为, 呈极度不平衡状态, 尤其是耕地和其他林地; 2010 年后各植被类型的趋势状态指数 P_i 减小, 说明单向转换变弱, 植被转换趋于稳定。耕地在空间转换上比较剧烈, 2000—2005 年耕地主要转换为其他林地和高覆盖度草地, 2005—2010 年主要转换为其他林地, 耕地面积逐步缩减, 表明 GGP 实施效果显著。2000—2005 年其他林地显著增加, 到 2005—2010 年变化速度显著减小, 但仍呈现极端不平衡态势, 但面积稳步增加, 后期逐渐趋于平稳。有林地、疏林地及灌木地在 2000—2005 年主要由中低覆盖度草地转化而来, 2005 年后面积逐步减少, 但总变化量小 (T_c 为 0.14%~2.66%)。草地的总减少量较 GGP 实施前整体变小, 说明草地面积缩减趋势已得到遏制。初期, 高覆盖度草地朝规模增大的方向发展, 处于不平衡态势, 以耕地转化为该类型为主, 后期趋于稳定, 双向转换频繁, P_i 接近 0。中低覆盖度草地整体处于减少趋势, 主要转换为其他用地, 但总变化量不大。

对整个研究时段 (1980—2015 年) 而言, 耕地面积显著减少 (约 1 012 km², $N_c = -2.84%$), 主要转换为其他林地, 高覆盖度草地和其他用地; 林地显著增加, 尤以其他林地的数量增加最多, 净变化速度最快 ($R_c = 4.22%$), 主要由耕地和中覆盖度草地转化

而来,灌木林和疏林地也主要由中覆盖度草地转化而来;高低覆盖度草地增加,中覆盖度草地显著减少(约 986 km², $N_c = -4.46\%$),高覆盖度草地和低覆

盖度草地处于平衡状态($P_s \leq 0.25$),中覆盖度草地主要转化为低覆盖度草地和其他用地;其他用地变化不显著,处于动态平衡状态($P_s \approx 0$)。

表 1 黄河中游河龙区间各植被类型变化量化指标

| 时段 | 耕地 | 有林地 | 灌木地 | 疏林地 | 其他林地 | 高覆盖度草地 | 中覆盖度草地 | 低覆盖度草地 | 其他用地 | |
|-------------|----------------------|--------|--------|--------|--------|--------|--------|--------|--------|--------|
| 1980—1990 年 | 面积变化/km ² | 355 | 28 | -33 | -63 | 15 | -110 | -58 | -81 | -65 |
| | 净变化 $N_c/\%$ | 1.00 | 0.98 | -0.37 | -1.80 | 5.54 | -2.76 | -0.26 | -0.35 | -0.57 |
| | 总变化 $T_c/\%$ | 103.92 | 103.96 | 94.21 | 133.30 | 161.99 | 119.78 | 99.97 | 103.64 | 93.56 |
| | 趋势状态指数 P_s | 0.01 | 0.01 | 0 | -0.01 | 0.03 | -0.02 | 0 | 0 | -0.01 |
| | 净变化速度 $R_s/\%$ | 0.10 | 0.10 | -0.04 | -0.18 | 0.54 | -0.28 | -0.03 | -0.04 | -0.06 |
| 1990—1995 年 | 面积变化/km ² | -37 | -621 | -397 | -359 | 39 | 135 | 4 526 | -1 253 | -2 030 |
| | 净变化 $N_c/\%$ | -0.10 | -21.55 | -4.52 | -10.45 | 13.64 | 3.48 | 20.55 | -5.48 | -18.04 |
| | 总变化 $T_c/\%$ | 102.87 | 122.07 | 107.75 | 145.11 | 175.17 | 139.78 | 130.16 | 121.72 | 88.90 |
| | 趋势状态指数 P_s | 0 | -0.18 | -0.04 | -0.07 | 0.08 | 0.02 | 0.16 | -0.04 | -0.20 |
| | 净变化速度 $R_s/\%$ | -0.02 | -4.74 | -0.92 | -2.18 | 2.59 | 0.69 | 3.81 | -1.12 | -3.90 |
| 1995—2000 年 | 面积变化/km ² | -133 | 549 | 508 | 496 | 5 | -279 | -4 769 | 2 615 | 1 016 |
| | 净变化 $N_c/\%$ | -0.37 | 24.28 | 6.05 | 16.12 | 1.54 | -6.95 | -17.96 | 12.09 | 11.01 |
| | 总变化 $T_c/\%$ | 104.15 | 161.96 | 118.31 | 170.46 | 172.62 | 140.48 | 110.07 | 131.79 | 108.75 |
| | 趋势状态指数 P_s | 0 | 0.15 | 0.05 | 0.09 | 0.01 | -0.05 | -0.16 | 0.09 | 0.10 |
| | 净变化速度 $R_s/\%$ | -0.07 | 4.44 | 1.18 | 3.03 | 0.31 | -1.43 | -3.88 | 2.31 | 2.11 |
| 2000—2005 年 | 面积变化/km ² | -1131 | 125 | 129 | 57 | 718 | 454 | -400 | -399 | 447 |
| | 净变化 $N_c/\%$ | -3.16 | 4.45 | 1.45 | 1.60 | 217.58 | 12.16 | -1.84 | -1.65 | 4.37 |
| | 总变化 $T_c/\%$ | 3.84 | 7.86 | 2.39 | 2.32 | 221.21 | 20.24 | 4.61 | 3.43 | 7.24 |
| | 趋势状态指数 P_s | -0.82 | 0.57 | 0.61 | 0.69 | 0.98 | 0.60 | -0.40 | -0.48 | 0.60 |
| | 净变化速度 $R_s/\%$ | -0.64 | 0.87 | 0.29 | 0.32 | 26.00 | 2.32 | -0.37 | -0.33 | 0.86 |
| 2005—2010 年 | 面积变化/km ² | -138 | 2 | -4 | 12 | 117 | 2 | -2 | 66 | -55 |
| | 净变化 $N_c/\%$ | -0.40 | 0.07 | -0.04 | 0.33 | 11.16 | 0.05 | -0.01 | 0.28 | -0.51 |
| | 总变化 $T_c/\%$ | 0.48 | 0.14 | 0.13 | 0.39 | 11.16 | 0.76 | 0.40 | 0.49 | 1.39 |
| | 趋势状态指数 P_s | -0.82 | 0.50 | -0.33 | 0.86 | 1.00 | 0.06 | -0.02 | 0.56 | -0.37 |
| | 净变化速度 $R_s/\%$ | -0.08 | 0.01 | -0.01 | 0.07 | 2.14 | 0.01 | 0 | 0.06 | -0.10 |
| 2010—2015 年 | 面积变化/km ² | 72 | 2 | -33 | -18 | -13 | -20 | -283 | -368 | 662 |
| | 净变化 $N_c/\%$ | 0.21 | 0.07 | -0.37 | -0.49 | -1.12 | -0.48 | -1.32 | -1.54 | 6.23 |
| | 总变化 $T_c/\%$ | 1.95 | 2.66 | 0.99 | 2.09 | 20.17 | 6.30 | 2.61 | 2.30 | 9.92 |
| | 趋势状态指数 P_s | 0.11 | 0.03 | -0.37 | -0.24 | -0.06 | -0.08 | -0.51 | -0.67 | 0.63 |
| | 净变化速度 $R_s/\%$ | 0.04 | 0.01 | -0.07 | -0.10 | -0.22 | -0.10 | -0.27 | -0.31 | 1.22 |
| 1980—2015 年 | 面积变化/km ² | -1 012 | 85 | 170 | 125 | 881 | 182 | -986 | 580 | -25 |
| | 净变化 $N_c/\%$ | -2.84 | 2.98 | 1.93 | 3.57 | 325.09 | 4.56 | -4.46 | 2.53 | -0.22 |
| | 总变化 $T_c/\%$ | 6.30 | 11.95 | 5.55 | 7.92 | 332.47 | 29.78 | 10.87 | 13.72 | 29.67 |
| | 趋势状态指数 P_s | -0.45 | 0.25 | 0.35 | 0.45 | 0.98 | 0.15 | -0.41 | 0.18 | -0.01 |
| | 净变化速度 $R_s/\%$ | -0.08 | 0.08 | 0.05 | 0.10 | 4.22 | 0.13 | -0.13 | 0.07 | -0.01 |

由综合状态趋势指数及综合净变化速度(表 2)可知,GGP 实施前,尤其是 1990—2000 年各植被类型转换速度较快($R_t \geq 0.83\%$),且相互转化剧烈($P_t \leq 0.08$),整体处于动态平衡状态;而 GGP 实施后转换速度明显减缓($R_t \leq 0.34\%$),且各植被类型间由不平衡状态($P_t = 0.65$)转化为准

平衡状态($P_t = 0.41$),各类型间单向转化剧烈。

综上可知,GGP 的实施显著地改变了河龙区间各植被类型的平衡状态。耕地不断减少,GGP 实施初期效果最为显著;林地逐步增加,尤以其他林地增加最多,但后期增加速度减缓;草地不断减少的趋势得到遏制;其他用地趋于稳定。

表 2 黄河中游河龙区间植被综合状态趋势指数及综合净变化速度

| 综合指标 | 1980—1990 年 | 1990—1995 年 | 1995—2000 年 | 2000—2005 年 | 2005—2010 年 | 2010—2015 年 | 1980—2015 年 |
|------------------|-------------|-------------|-------------|-------------|-------------|-------------|-------------|
| 总体面积净变化 $S_a/\%$ | 0.36 | 4.22 | 4.65 | 1.73 | 0.18 | 0.66 | 1.82 |
| 总变化 $S_s/\%$ | 51.45 | 57.19 | 58.44 | 2.67 | 0.31 | 1.61 | 6.44 |
| 总趋势与状态指数 P_t | 0.01 | 0.07 | 0.08 | 0.65 | 0.57 | 0.41 | 0.28 |
| 总净变化速度 $R_t/\%$ | 0.04 | 0.83 | 0.91 | 0.34 | 0.04 | 0.13 | 0.05 |

2.3 植被变化对径流的影响

植被变化主要通过改变流域下垫面条件,进而影响“降水-下渗-蒸散发-径流”的水循环过程^[3]。由以上定量分析可知,1980 年以来该流域内植被类型的转化方向发生了显著变化,特别是 1999 年 GGP 的实施,使得 2000—2016 年各植被类型以单向转化为主,呈现不平衡状态。此外,该流域内地形、地貌和土壤特性较为稳定,所以该流域下垫面的变化主要体现为植被的变化。为了量化植被对径流的影响,本文基于布迪克弹性系数法^[27],评估径流对植被的响应。

表 3 显示了河龙区间不同时段水文气象特征,以及下垫面参数 n 的变化和对径流的影响。由表 3 可知,多年平均径流深在 GGP 实施前(1980—1999 年)为 38.5 mm,而在 GGP 实施后的 10 年(2000—2010 年),尽管降水量呈现增加趋势,但径流深呈急剧

下降趋势,2000—2005 年相较前一时段下降 7.2 mm,2006—2010 年则下降到 21.8 mm,较 GGP 实施前下降了 43.4%。对应时期的下垫面参数 n 在 GGP 实施前为 2.05,实施后增加到 2.51。其中,2000—2005 年 n 增加为 2.19,GGP 实施所引起的下垫面植被变化对径流的贡献率为 91.0%,2006—2010 年 n 达到了 2.65,较 GGP 实施前增加了 29.3%且植被对径流的贡献率高达 193.7%。与下垫面参数 n 反应的结果一致,植被的增加对应径流的减小,表明植被对径流的影响程度进一步加强。所以,植被变化成为 GGP 实施后 10 年径流下降主要影响因素。2011—2016 年下垫面参数 n 变为 2.77,而降水持续增加,相较 2006—2010 年增加了 57 mm,植被对径流的影响减小,其对径流的贡献率减小为-38.6%,降水成为影响径流的主要因素,使得径流增加至 38.2 mm。

表 3 河龙区间不同时段水文气象要素以及植被对径流贡献

| 时间区间 | 径流 | 降水 | 潜在蒸散发 | 参数 n | 弹性系数 | 贡献量 | 贡献率/% |
|-------------|------|-------|-------|--------|-------|--------|-------|
| 1980—1999 年 | 38.5 | 448.2 | 975 | 2.05 | -2.35 | | |
| 2000—2005 年 | 31.3 | 446.0 | 993 | 2.19 | -2.53 | -6.55 | 91.0 |
| 2006—2010 年 | 21.8 | 465.9 | 990 | 2.65 | -2.81 | -18.40 | 193.7 |
| 2011—2016 年 | 28.5 | 522.9 | 994 | 2.77 | -2.58 | -2.60 | -38.6 |
| 2000—2016 年 | 27.5 | 479.0 | 992 | 2.51 | -2.62 | -22.62 | 206.2 |

注:弹性系数是指径流对植被参数 n 的弹性系数,贡献量指植被对径流的贡献量,2000 年后的各个时段相对上一个时段而言。

由以上分析可知,GGP 实施后的 2000—2010 年,下垫面参数 n 增加显著,植被对径流的贡献率显著增加,径流急剧下降,植被变化成为该流域径流下降的主要因素。随着 2011—2016 年降水的持续增加,植被对径流的影响减小,降水成为该流域径流增加的主要因素,径流深呈现增加趋势。

为了进一步分析 1980—2016 年河龙区间植被变化与径流关系,利用 Mann-Kendall 检验法对径流进行了突变点检测(图 3(b))。可以看出径流的突变点大约位于 2004 年,为退耕还林工程实施后的第 5 年,表明植被恢复的效应初显。径流深由转折点前的 37.4 mm/a,下降到 26 mm/a,下降幅度为 30.5%(图 3(a))。与本文发现结果类似,有研究指出黄土高原地区的退耕还林工程减少了区域的水资

源可利用量^[5,23]。然而,尽管径流深在 2004—2010 年呈下降趋势(-2.3 mm/a, $p < 0.01$),但在 2011—2016 年,径流深呈现增加趋势(4.6 mm/a, $p < 0.1$)。与转折点前相比,转折点后的径流系数(径流深/降水量)下降(图 3(c)),表明流域植被覆盖率增加,改变了下垫面条件,导致地表反照率减少,地表净辐射能量增加,植被通过蒸散发消耗这部分能量^[28]。降水量变化不大时,较高的蒸散发量会导致径流系数减少,使得流域整体产流能力下降,故而该流域的植被变化已显著地改变了“降水-下渗-蒸散发-径流”的水文过程。然而,2011—2016 年河龙区间植被覆盖面积持续增加,随着降水量持续增加,流域产流能力也持续增加。干燥指数是水热状况的指标,可反映较长时间尺度一个区域的气候特

征^[29-30]。河龙区间的干燥指数(图3(d))由2.22(1980—2004年)下降到2.10(2004—2016年),特别是

2011—2016年随着降水的增加,干燥指数达到了1.93,整体呈现“变湿”的趋势。

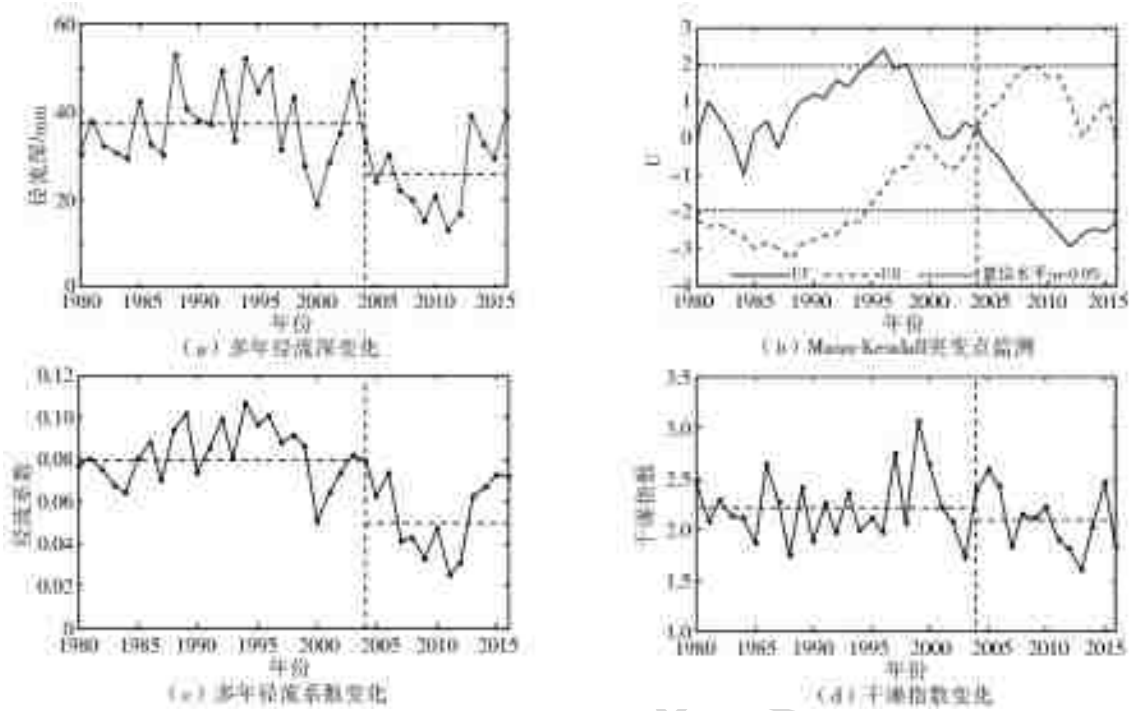


图3 黄河中游河龙区间径流突变点检测、径流系数和干燥指数特征

3 结论

本文利用7期植被类型数据、径流资料和气象数据,基于植被变化的量化模型,分析了1980—2015年黄河中游河龙区间植被时空动态,并利用基于布迪克理论框架的弹性系数法,阐明了植被对径流变化的影响。结果表明,GGP的实施并没有显著改变河龙区间各植被类型的空间分布格局,但显著改变了各植被类型的平衡状态及不同类型间的转换速度和方向。各植被类型从GGP实施前的动态平衡,双向转换频繁转变为GGP实施后的不平衡,单向转换为主,其中以耕地转化为其他林地和高覆盖度草地为主,使得草地面积缩减趋势得到遏制,后期变化速度减缓,各种植被类型趋于稳定。河龙区间GGP实施导致的植被变化对径流产生了显著影响,植被变化是GGP实施后10年内径流下降的主要原因,其后降水不断增加,其“减水效应”也趋于缓和。加强黄河中游河龙区间植被变化格局的定量研究,及其对径流变化的影响研究,可为植被恢复工程的实施、流域水资源的开发利用提供参考依据。

参考文献:

[1] PIAO S, YIN G, TAN J, et al. Detection and attribution of vegetation greening trend in China over the last 30 years[J]. *Global Change Biology*, 2015, 21(4): 1601-

1609. DOI:10.1111/gcb.12795.
 [2] FENG X, FU B, PIAO S, et al. Revegetation in China's Loess Plateau is approaching sustainable water resource limits[J]. *Nature Climate Change*, 2016, 6(11): 1019-1022. DOI:10.1038/nclimate3092.
 [3] JACKSON R B. Trading water for carbon with biological carbon sequestration[J]. *Science*, 2005, 310(5756): 1944-1947. DOI:10.1126/science.1119282.
 [4] PIAO S, CIAIS P, HUANG Y, et al. The impacts of climate change on water resources and agriculture in China[J]. *Nature*, 2010, 467(7311): 43-51. DOI:10.1038/nature09364.
 [5] SUN G, ZHOU G, ZHANG Z, et al. Potential water yield reduction due to forestation across China[J]. *Journal of Hydrology*, 2006, 328(3-4): 548-558. DOI:10.1016/j.jhydrol.2005.12.013.
 [6] 梁伟,杨勤科. 基于RS的黄河中游多沙粗沙区土地利用变化分析[J]. *水土保持研究*, 2006, 13(5): 90-92. DOI:10.3969/j.issn.1005-3409.2006.05.030.
 [7] 李滚,梁伟,杨勤科. 黄河中游多沙粗沙区土地利用格局变化分析[J]. *中国水土保持科学*, 2009, 7(3): 52-58. DOI:10.3969/j.issn.1672-3007.2009.03.010.
 [8] 周德成,赵淑清,朱超. 退耕还林工程对黄土高原土地利用/覆被变化的影响-以陕西省安塞县为例[J]. *自然资源学报*, 2011, 26(11): 1866-1878. DOI:10.11849/zrzyxb.2011.11.006.
 [9] 刘昌明,李艳忠,刘小莽,等. 黄河中游植被变化对水量

- 转化的影响分析[J]. 人民黄河, 2016, 38(10): 7-12. DOI: 10. 3969/j. issn. 1000-1379. 2016. 10. 002.
- [10] 刘昌明, 钟骏襄. 黄土高原森林对年径流影响的初步分析[J]. 地理学报, 1978, 33(2): 112-127. DOI: 10. 11821/xb197802003.
- [11] CAO S, CHEN L, YU X. Impact of China's Grain for Green Project on the landscape of vulnerable arid and semi-arid agricultural regions; a case study in northern Shaanxi Province [J]. *Journal of Applied Ecology*, 2009, 46(3): 536-543. DOI: 10. 1111/j. 1365-2664. 2008. 01605. x.
- [12] CHEN Y. Balancing green and grain trade [J]. *Nature Geoscience*, 2015, 8(10): 739-741. DOI: 10. 1038/ngeo2544.
- [13] MCVICAR T R, LI L T, NIEL T G V, et al. Developing a decision support tool for China's re-vegetation program; Simulating regional impacts of afforestation on average annual streamflow in the Loess Plateau [J]. *Forest Ecology and Management*, 2007, 251(1): 65-81. DOI: 10. 1016/j. foreco. 2007. 06. 025.
- [14] 杨胜天, 周旭, 刘晓燕, 等. 黄河中游多沙粗沙区(渭河段)土地利用对植被盖度的影响[J]. 地理学报, 2014, 75(1): 31-41. DOI: 10. 11821/dlxb201401003.
- [15] 李艳忠, 刘昌明, 刘小莽, 等. 植被恢复工程对黄河中游土地利用/覆被变化的影响[J]. 自然资源学报, 2016, 31(12): 2005-2020. DOI: CNKI: SUN: ZRZX. 0. 2016-12-004.
- [16] LI Y, LIU C, ZHANG D, et al. Reduced runoff due to anthropogenic intervention in the Loess Plateau, China [J]. *Water*, 2016, 8(458): 1-16. DOI: 10. 3390/w8100458.
- [17] LIANG K, LIU C, LIU X, et al. Impacts of climate variability and human activity on streamflow decrease in a sediment concentrated region in the Middle Yellow River [J]. *Stochastic Environmental Research & Risk Assessment*, 2013, 27(7): 1741-1749. DOI: 10. 1007/s00477-013-0713-2.
- [18] FATHIAN F, DEHGHAN Z, BAZRKAR M H, et al. Trends in hydrologic and climatic variables affected by four variations of Mann-Kendall approach in Urmia Lake basin, Iran [J]. *Hydrological Sciences Journal*, 2016, 61(5): 892-904. DOI: 10. 1080/02626667. 2014. 932911.
- [19] ALLEN R G, PEREIRA L S, RAES D, et al. Crop evapotranspiration-Guidelines for computing crop water requirements-FAO Irrigation and drainage paper 56 [M]. FAO, 1998. DOI: 10. 1007/978-3-319-05699-9_6.
- [20] LIU X, LIU W, XIA J. Comparison of the streamflow sensitivity to aridity index between the Danjiangkou Reservoir basin and Miyun Reservoir basin, China [J]. *Theoretical and Applied Climatology*, 2013, 111(3-4): 683-691. DOI: 10. 1007/s00704-012-0701-3.
- [21] MCCUEN R H. A sensitivity and error analysis of procedures used for estimating evaporation [J]. *Journal of the American Water Resources Association*, 1974, 10(3): 486-497. DOI: 10. 1111/j. 1752-1688. 1974. tb00590. x.
- [22] CONG Z, SHAHID M, ZHANG D, et al. Attribution of runoff change in the alpine basin; a case study of the Heihe Upstream basin, China [J]. *Hydrological Sciences Journal*, 2017, 62(6): 1013-1028. DOI: 10. 1080/02626667. 2017. 1283043.
- [23] LIANG W, BAI D, WANG F, et al. Quantifying the impacts of climate change and ecological restoration on streamflow changes based on a Budyko hydrological model in China's Loess Plateau [J]. *Water Resources Research*, 2015, 51(8): 6500-6519. DOI: 10. 1002/2014wr016589.
- [24] 杨大文, 张树磊, 徐翔宇. 基于水热耦合平衡方程的黄河流域径流变化归因分析[J]. 中国科学: 技术科学, 2015, 45(10): 1024-1034. DOI: 10. 1360/N092015-00013.
- [25] RODERICK M L, FARQUHAR G D. A simple framework for relating variations in runoff to variations in climatic conditions and catchment properties [J]. *Water Resources Research*, 2011, 47(12). DOI: 10. 1029/2010WR009826.
- [26] ZHANG S, YANG H, YANG D, et al. Quantifying the effect of vegetation change on the regional water balance within the Budyko framework [J]. *Geophysical Research Letters*, 2015, 43(3): 1140-1148. DOI: 10. 1002/2015GL066952.
- [27] LIU X M, LUO Y Z, ZHANG D, et al. Recent changes in pan-evaporation dynamics in China [J]. *Geophysical Research Letters*, 2011, 38(38): 142-154. DOI: 10. 1029/2011gl047929.
- [28] MYKLEBY P M, LENTERS J D, Cutrell G J, et al. Energy and water balance response of a vegetated wetland to herbicide treatment of invasive phragmites australis [J]. *Journal of Hydrology*, 2016, 539: 290-303. DOI: 10. 1016/j. jhydrol. 2016. 05. 015.
- [29] LIU X, ZHANG D, LUO Y, et al. Spatial and temporal changes in aridity index in northwest China: 1960 to 2010 [J]. *Theoretical and applied climatology*. 2013, 112(1-2): 307-316. DOI: 10. 1007/s00704-012-0734-7.
- [30] LI Y, FENG A, LIU W, et al. Variation of aridity index and the role of climate variables in the southwest China [J]. *Water*, 2017, 9(10): 743. DOI: 10. 3390/w9100743.

• 译文(Translation) •

DOI: 10.13476/j.cnki.nsbdkj.2020.0054

Vegetation dynamics and its impact on runoff in the Hekouzhen-Longmen region of the middle reaches in the Yellow River from 1980 to 2016

ZHANG Jianmei¹, MA Xieyao², LI Yanzhong²

(1. School of Atmospheric Science, Nanjing University of Information Science and Technology, Nanjing 210044, China;

2. School of Hydrology and Water Resources, Nanjing University of Information Science and Technology, Nanjing 210044, China)

Abstract: The Hekouzhen-Longmen region of the middle reaches in the Yellow River is a key and typical area for the implementation of the Grain for Green Project (GGP) in China. It is of great significance for the sustainable utilization of water resources and the eco-hydrological effect assessment of the GGP project to quantitatively evaluate the vegetation dynamics and its impact on runoff in the basin. Based on remote sensing, GIS technology, mathematical statistics, and Budyko framework, the spatial-temporal change pattern of vegetation cover and its impact on runoff change is quantitatively evaluated using different vegetation type data of seven periods in the Hekouzhen-Longmen region for past 37 years. The results indicate that; 1) the change in vegetation do not significantly change the temporal and spatial distribution pattern of each vegetation type in the Hekouzhen-Longmen region; 2) the implementation of the GGP change the equilibrium status and transformation rate of each vegetation type; 3) vegetation changes are the main driving factor of runoff decline after the implementation of GGP in the last 10 years (2000-2010), but the subsequent continuous increase in precipitation make the "water reduction effect" of vegetation tend to ease.

Key words: middle reaches of the Yellow River; the Hekouzhen-Longmen region; vegetation change; Grain for Green Project; contribution to streamflow

Vegetation change, as one of the main forms of land use/cover change (LUCC), can affect the re-distribution of water and energy. In recent years, regional and global scale vegetation changes have been widely concerned and reported^[1-2], especially the changes in vegetation caused by severe human activities have produced relatively severe variations in terrestrial water resources distribution patterns, water cycle processes and carbon cycles^[3-4]. In order to achieve the goal of "rebuilding a beautiful

northwestern region with mountains and rivers", our government has implemented several vegetation restoration projects among which the Grain for Green Project (GGP) implemented in 1999, is the largest vegetation restoration project executed in a developing country. The implementation of this project has a direct impact on regional and national scale vegetation changes and sustainable use of resources and the environment^[5]. Therefore, quantitative assessment of the impact of GGP implemen-

Received: 2019-09-10 Revised: 2019-10-30 Online publishing: 2019-11-25

Online publishing address: <http://kns.cnki.net/kcms/detail/13.1334.TV.20191125.1148.002.html>

Author brief: ZHANG Jianmei (1995-), female, born in Nantong, Jiangsu Province, is mainly engaged in regional climate change, hydrological and water resources research. E-mail: 18252088753@163.com

Corresponding author: MA Xieyao (1963-), male, Ningbo, Zhejiang Province, professor, Ph. D., mainly engaged in in climate change and hydrological research. E-mail: xyyma@nuist.edu.cn

tation on vegetation dynamic and pattern, as well as the influence of vegetation change on runoff alteration, may help to better understand the ecological and hydrological effects of vegetation and to formulate ecological restoration measures.

The middle reaches of the Yellow River are located in the semi-arid and semi-humid transition zone of China. The soil and water loss, flood disasters, and deterioration of the water environment are more serious in the region. It is a key area for vegetation restoration projects. Many scholars have studied the changes of vegetation in the middle reaches of the Yellow River. For example, Liang Wei et al.^[6] analyzed the land use changes in the sandy and coarse areas of the middle reach of the Yellow River using remote sensing images from 1975, 1986, and 1997. They found that cultivated land, forestland, and grassland are the leading type of land use change before the implementation of GGP. Li Gun et al.^[7] used the land use data for the years 1977, 1997, and 2006 to investigate the change rate of farmland, grassland, forestland, unused land, and their transfer rates. The change rate and transfer rate of land, forestland and unused land are greatly affected by the policy of returning farmland to a forest (grass), among which the forestland area continues to increase, the cultivated land and unused land decrease, and the grassland first decreases and then increases, respectively. Zhou Decheng et al.^[8] used the LUCC data from 1978-2010 to study the influence of GGP on all kinds of areas in Ansai County, Hekouzhen-Longmen region and found that GGP developed an unbalanced situation in the study area. The cultivated land first increased and then decreased, the forestland decreased and then increased, while the shrubland and grassland decreased. Liu Changming et al.^[9] found that leaf area index (LAI) and normalized vegetation index (NDVI) of 11 sub-basins in the middle reaches of the Yellow River increased in 2000, with the most significant change in the Hekouzhen-Longmen region. However, the quantitative analysis of vegetation patterns in 2000-2015 is relatively weak in the middle reaches of the Yellow River, especially the significant vegetation change

in the Hekouzhen-Longmen region. Scholars have also carried out a lot of research work for impact assessment of vegetation change on runoff in the middle reaches of the Yellow River. For example, Liu Changming and Zhong Junxiang^[10] found that the increase of forest in the middle reaches of the Yellow River reduced the annual runoff, decreased the flood flow, increased the groundwater runoff, and thus changed the process of runoff distribution. Cao et al.^[11] believed that large-scale afforestation activities may exacerbate water shortages in semi-arid and semi-humid areas, and eventually lead to a reduction in afforestation survival rate and vegetation coverage. Chen et al.^[12] documented that if the vegetation in the Loess Plateau continues to change, the available water resources will be reduced. However, there are few studies regarding the effects of vegetation changes on runoff in the key areas of the vegetation restoration project-Hekouzhen-Longmen region, especially after 2010.

Based on aforementioned context, this paper selects the Hekouzhen-Longmen region as the study area and uses the 7 periods of land use data (the late 1980s to 2015), and hydrometeorological data such as precipitation and runoff to conduct a dynamic analysis of the spatial distribution pattern of vegetation, quantitative assessment, and analysis of the contribution of vegetation changes to runoff, aiming to reveal the temporal and spatial distribution of vegetation in the study area. In order to understand the dynamic process of vegetation change in the middle reaches of the Yellow River and provide a reference for the evaluation of the effect of GGP, this paper quantitatively assesses the impact of GGP on the direction, change rate, and trend of vegetation changes in the Hekouzhen-Longmen region, and clarify the effects of vegetation changes on runoff.

1 Research area and method

1.1 Overview of the study area

The study area is situated in the Hekouzhen-Longmen region, namely, the area from Hekou Town to Longmen. The catchment area is 11.2 thousand km², accounting for 14.8% of the total

drainage area of the Yellow River. This area is located in the semi-arid and semi-humid transition zone of China, belonging to the temperate continental monsoon climate. The precipitation decreases from the southeast to the northwest with significant spatial distribution differences and uneven seasonal distribution. It is mainly concentrated in June to September, making the Hekouzhen-Longmen region a most severe soil erosion region of the Yellow River basin^[13-14]. The average annual rainfall in the area is about 451.7 mm and the evaporation measured by the pan evaporation is about 1 500 mm, respectively^[15]. The hills are widely distributed, the terrain is high in the north and west and low in the south and east, low in the middle, and the altitude is mostly between 1 000-1 500 m.

1.2 Data

In this paper, the data of vegetation types of seven periods from the late 1980s, 1990, 1995, 2000, 2005, 2010, 2015 with a spatial resolution of 1 km are obtained from the data-sharing center of the Institute of Geosciences and resources, Chinese Academy of Sciences (<http://www.resdc.cn/>). According to the characteristics of the vegetation in the study area and the differences in landscape changes, referring to the "Technical Specifications for the Investigation of Land Use Status", the land use types are recombined and divided into 9 types such as cultivated land, forested land, shrubland, sparse forestland, other woodlands, high coverage grassland, medium coverage grassland, low coverage grassland, and other land use.

Meteorological data such as precipitation, temperature and wind speed for the period of 1980-2016 are extracted from the National Meteorological Information Center of the China Meteorological Administration (<http://data.cma.cn/>). The annual runoff data from 1980 to 1997 is obtained from the monthly runoff data compiled by the National Hydrological Yearbook, while the annual runoff data from 1998 to 2016 is extracted from the Yellow River Water Resources Bulletin (<http://www.yellowriver.gov.cn/other/hhgb/>). In order to eliminate the impact of human activities (field

irrigation, industry, residential life, urban public, etc.) in the runoff, in this paper, the reduction runoff that ignores the impact of human activities is used^[16-17].

1.3 Research methods

1.3.1 Quantitative model of vegetation change

The spatial analysis module in ArcGIS 10.2 and ENVI 5.3 is used to perform the statistical and the overlay analysis for the 7th periodical vegetation types. The dynamic change degree and the vegetation cover change in the Hekouzhen-Longmen region are analyzed based on the area transfer matrix of each vegetation type for the last 35 years. The main indicators involved in the model are as follows^[8,15]

N_c , T_c , P_s , and R_s are the net change, total change trend, state index and net change rate of single vegetation type, respectively.

$$N_c = \frac{U_b - U_a}{U_a} \times 100\% = \frac{\Delta U_{in} - \Delta U_{out}}{U_a} \times 100\% \quad (1)$$

$$T_c = \frac{\Delta U_{in} + \Delta U_{out}}{U_a} \times 100\% \quad (2)$$

$$P_s = \frac{N_c}{T_c} = \frac{\Delta U_{in} - \Delta U_{out}}{\Delta U_{in} + \Delta U_{out}} \quad (3)$$

$$R_s = (\sqrt[T]{\frac{U_b}{U_a}} - 1) \times 100\% =$$

$$\left[\sqrt[T]{\frac{U_a + (\Delta U_{in} - \Delta U_{out})}{U_a}} - 1 \right] \times 100\% \quad (4)$$

S_a , S_s , P_t , and R_t are the net change, total change, trend and status index, and net change rate of the total vegetation area, respectively.

$$S_a = \frac{\sum_{i=1}^n |U_{bi} - U_{ai}|}{2 \sum_{i=1}^n U_{ai}} \times 100\% =$$

$$\frac{\sum_{i=1}^n |U_{in-i} - U_{out-i}|}{2 \sum_{i=1}^n U_{ai}} \times 100\% \quad (5)$$

$$S_s = \frac{\sum_{i=1}^n |U_{in-i} + U_{out-i}|}{2 \sum_{i=1}^n U_{ai}} \times 100\% =$$

$$\frac{\sum_{i=1}^n \Delta U_{out-i}}{\sum_{i=1}^n U_{ai}} \times 100\% = \frac{\sum_{i=1}^n \Delta U_{in-i}}{\sum_{i=1}^n U_{ai}} \times 100\% \quad (6)$$

$$P_t = \frac{S_a}{S_s} = \frac{\sum_{i=1}^n |U_{out-i} - U_{in-i}|}{\sum_{i=1}^n |U_{out-i} + U_{in-i}|}, 0 \leq \frac{S_a}{S_s} \leq 1 \text{ 且}$$

$$0 \leq P_t \leq 1, S_s \neq 0 \quad (7)$$

$$R_t = \left[\frac{\sum_{i=1}^n U_{a-i} + \frac{1}{2} \sum_{i=1}^n |U_{b-i} - U_{a-i}|}{\sum_{i=1}^n U_{a-i}} - 1 \right] \times 100\% = \left[\frac{\sum_{i=1}^n U_{a-i} + \frac{1}{2} \sum_{i=1}^n |U_{in-i} - U_{out-i}|}{\sum_{i=1}^n U_{a-i}} - 1 \right] \times 100\% \quad (8)$$

where U_a and U_b are the areas of a certain vegetation type at the beginning and end of the study period; U_{out} is the sum of the areas of a certain vegetation type converted to other vegetation types during the study period; U_{in} is the sum of the area of other vegetation types transformed into that vegetation type in the same period; U_{a-i} and U_{b-i} are the areas of the i -th vegetation type at the beginning and end of the study period; U_{out-i} is the sum of the area of the i -th vegetation type changed to other vegetation types during the study period; U_{in-i} is the sum of the areas of vegetation types changed into type i ; n is the total number of vegetation types; T is the study period.

1.3.2 Mutation points detection and potential evapotranspiration calculation

The non-parametric Mann-Kendall method is used to detect the mutation points in the runoff time series. This method is a commonly used method to test non-parametric statistics. It can test linear or non-linear trends and is often used for the change analysis of hydrological and meteorological variable series^[18].

The potential evapotranspiration is obtained using the reference crop evapotranspiration calculation method^[19]:

$$ET_0 = \frac{0.408\Delta(R_n - G) + \gamma \frac{900}{T_a + 273} u_2 \cdot VPD}{\Delta + \gamma(1 + 0.34u_2)} \quad (9)$$

where ET_0 is the daily potential evapotranspiration (mm/d), Δ is the slope of the temperature-saturated water vapor pressure curve (kPa/°C), R_n is the net surface radiation (MJ/(m² · d)), and G is the soil heat flux (MJ/(m² · d)), γ is the wet and dry bulb constant (kPa/°C), T_a is the average daily temperature (°C) at a height of 2 m, and u_2 is the wind speed (m / s) at a height of 2 m, VPD is the water vapor pressure difference (kPa).

1.3.3 Quantitative model for vegetation impact on runoff

The elastic coefficient is defined as the ratio of the change rate of the dependent variable to the change rate of the independent variable and is often used as the sensitivity index of one variable to another^[20-21]. The elasticity of runoff to other factors can be expressed as;

$$E_x = \lim_{\Delta x/x} \left[\frac{\Delta R/R}{\Delta x/x} \right] = \frac{\partial R}{\partial x} \times \frac{x}{R} \quad (10)$$

where E_x is the elastic coefficient; R is the runoff; x is a specific factor, such as precipitation, potential evapotranspiration, etc.

For a closed watershed, the actual evapotranspiration ET_a can be estimated by the water balance equation.

$$ET_a = P - Q - \Delta S \quad (11)$$

where ET_a is the actual evapotranspiration (mm); P is the precipitation in (mm), and is the change of soil water storage (mm). For a longer time scale (more than 5 years), the change in soil water storage is considered unchanged (i. e., $\Delta S \approx 0$), and formula (11) can be simplified as;

$$ET_a = P - Q \quad (12)$$

The long-term actual evapotranspiration ET_a can be estimated by Budyko's theoretical method, which has been used as an effective means to assess the correlation and feedback of climate and underlying surface changes^[22,23]. The most widely used model is Choudhury-Yang^[23-25]:

$$ET_a = \frac{P \cdot ET_0}{(P^n + ET_0^n)^{1/n}} \quad (13)$$

where P is the precipitation; n is a parameter reflecting the characteristics of the underlying surface of the watershed, such as terrain, landform, soil, and vegetation. The study found that when the topography and other factors change a little, the parameter n is closely related to vegetation change^[26], and can be estimated by vegetation index. Runoff change can be regarded as the total differential of precipitation, potential evapotranspiration and underlying surface parameter n , while the contribution of vegetation to runoff change (Cr_n) can be expressed as:

$$Cr_n = \epsilon_n \frac{\Delta n}{n} R \quad (14)$$

$$\epsilon_n = \frac{\ln(1+\varphi^n) + \varphi^n \ln(1+\varphi^{-n})}{n[(1+\varphi^n) - (1+\varphi^{-n})^{1/n+1}]} \quad (15)$$

where ϵ_n is the elastic coefficient of runoff to the underlying surface parameter $\varphi = ET_0/P$.

2 Research results

2.1 Spatial distribution of vegetation dynamics

Fig. 1 shows the spatial distribution of vegetation in the 7 periods from 1980 to 2015 in the Hekouzhen-Longmen region, while Fig. 2 lists the

statistical information of the area proportion of each vegetation type. It can be seen from Fig. 1 that there is no significant spatial difference among vegetation types in different periods in the study area. The statistical information in Fig. 2 revealed that the largest vegetation types in each period of the entire study area are cultivated land (range of 31.0% to 32.3%), followed by low-coverage grasslands (19.4% to 21.8%) and medium-coverage grasslands (18.9% to 23.8%), shrub forest (7.5% to 8.1%), high-coverage grassland (3.4% to

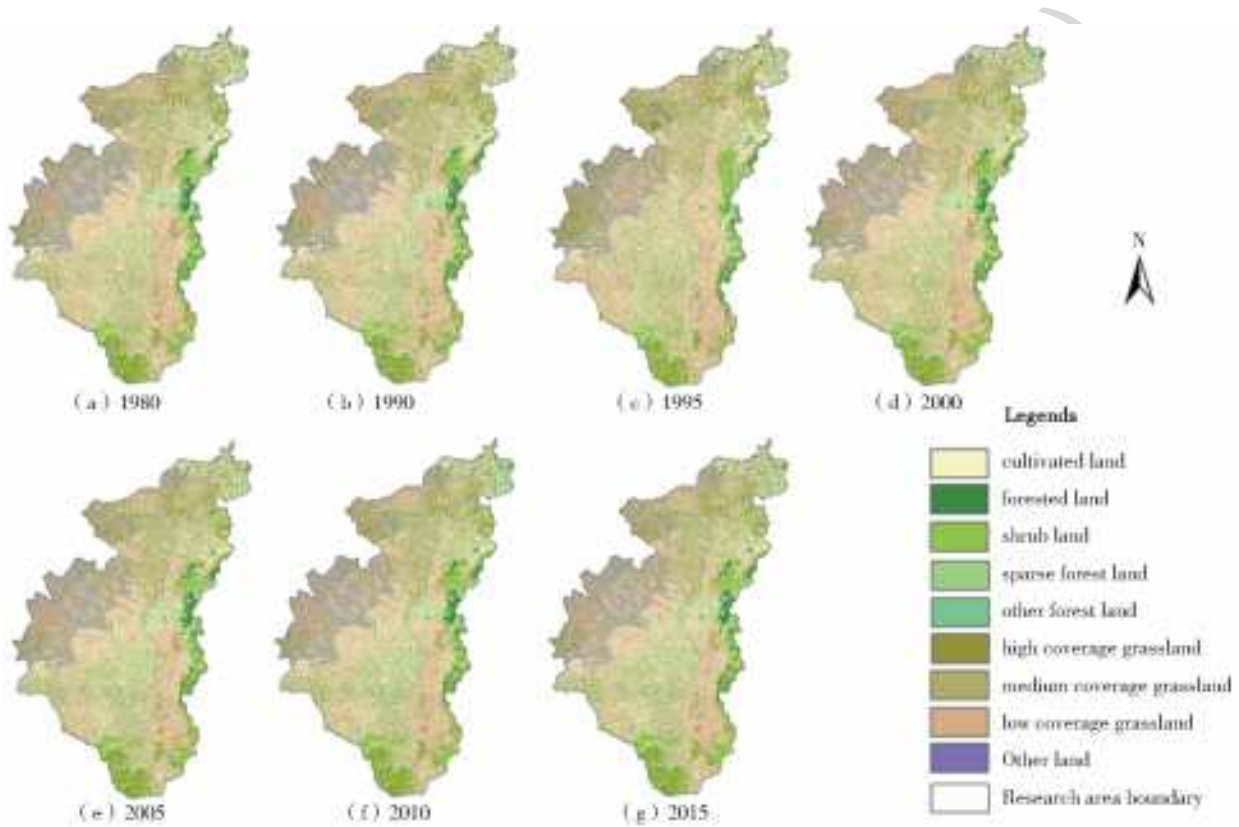


Fig. 1 Spatial distribution of LUCC in the Hekouzhen-Longmen region of the middle reaches in the Yellow River during 1980-2015

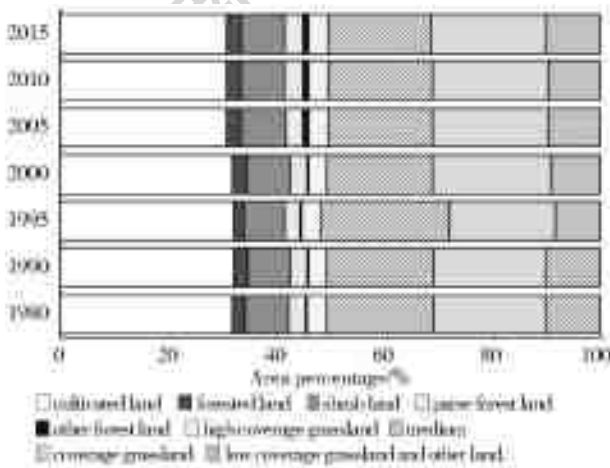


Fig. 2 The percentage of each vegetation type in the Hekouzhen-Longmen region of the middle reaches in the Yellow River

3.8%), and sparse woodland (2.8% to 3.3%), respectively. The smallest vegetation types are forestland and other woodlands (change range is 2.3% to 3.7%). It is concluded that GGP does not significantly change the spatial distribution pattern of vegetation types.

2.2 Quantitative assessment of vegetation changes

The implementation of GGP has altered the change rate and balance of the vegetation types in the river basin. According to Tab. 1, before the implementation of GGP, the trend state index P_s of

each vegetation type is small in the three stages (1980-1990, 1990-1995, and 1995-2000), indicating that each vegetation type is in a dynamic equilibrium state. The total change of cultivated land, forestland, and grassland is large (T_c is greater than 100%), but the quantity has not changed greatly, which shows that the three types of vegetation are relatively violent in spatial conversion, mainly due to the continuous large-scale reclamation of forestland and grassland as farmland, which results in the form of soil fertility decreases with the increase of the cultivation period^[15].

Likewise, after the implementation of GGP, in the three periods (2000-2005, 2005-2010 and 2010-2015), the absolute value of the trend state index P_s of each vegetation type increased from 2000 to 2010, indicating that each vegetation type is dominated by one-way conversion, showing an extremely unbalanced state, especially cultivated land and other woodlands. After 2010, the trend state index P_s of each vegetation type decrease, indicating that one-way conversion becomes weak, and the vegetation conversion has stabilized. From 2000 to 2005, the cultivated land is mainly converted to other woodlands and high-coverage grassland. Similarly, from 2005 to 2010, the cultivated land area is gradually reduced, indicating that the implementation effect of GGP is significant. From 2000 to 2005, other woodlands increased significantly, and the change rate decreased significantly from 2005 to 2010, but it is still showing an extremely unbalanced situation, because the area is increased steadily, and then gradually becomes stable. From 2000 to 2005, the forestland, sparse forestland and shrubland are mainly transformed from low-medium coverage grassland. After 2005, the area decreased gradually, but the total change is small (T_c was 0.14%–2.66%). The total reduction of grassland is smaller than that before the implementation of GGP, indicating that the reduction of the grassland area has been curbed. In the early stage, the high-coverage grassland developed in the direction of increasing scale and is in an unbalanced situation. The cultivated land is mainly transformed into this type. In the later stage, it tended to be stable, with frequent bidirectional

conversion and P_s close to 0. The grassland with low and medium coverage is in a decreasing trend as a whole, and it is mainly converted to other land use, but the total change is not large.

For the entire research period (1980-2015), the cultivated land area decreased significantly (about 1 012 km², $N_c = -2.84\%$), mainly converted to other woodlands, high coverage grassland, and other land use. The forestland increased significantly, especially the other forestland increased the most. The net change rate is fastest ($R_s = 4.22\%$), mainly from the cultivated land and medium coverage grassland, shrub and sparse forestland. It is mainly transformed from medium coverage grassland. The grassland with medium coverage decreased significantly (approximately 986 km², $N_c = -4.46\%$), the grassland with high coverage and grass with low coverage is in equilibrium ($P_s \leq 0.25$), and the grassland with medium coverage is mainly converted into the grass with low coverage and other land use. The results revealed that the other land use changes are not significant and are in a state of dynamic equilibrium ($P_s \approx 0$).

It can be seen from the total state trend index and the composite net change rate (Tab. 2) that before the implementation of GGP, especially from 1990 to 2000, the conversion rate of vegetation types is relatively fast ($R_t \geq 0.83\%$), and the mutual conversion is intense ($P_t \leq 0.08$), and the entire is in a state of dynamic balance. After the implementation of GGP, the conversion speed slow down significantly ($R_t \leq 0.34\%$), and the conversion of vegetation types is from the unbalanced state ($P_t = 0.65$). It is a quasi-equilibrium state ($P_t = 0.41$), while the one-way transformation between different types is intense.

In summary, the implementation of GGP has significantly changed the balance of various vegetation types in the Hekouzhen-Longmen region. Cultivated land is continuously decreasing, and the initial effect of GGP is most significant. Forestland is gradually increasing, especially other woodlands, but the increase rate is slowing in the later period. The decreasing trend of grassland is curbed while the other land is becoming stable.

Tab. 1 Quantitative indicators of changes in vegetation types in the Hekouzhen-Longmen region of the middle reaches in the Yellow river

| Period | | Cultiva ted land | Forestl and | Shrubl- and | Sparse forestland | Other woodl- ands | High Coverage grassland | Medium coverage grassland | Low coverage grassland | Other land use |
|-----------|--------------------------------|---------------------|----------------|----------------|----------------------|-------------------------|-------------------------------|---------------------------------|------------------------------|----------------------|
| 1980—1990 | Area variation/km ² | 355 | 28 | -33 | -63 | 15 | -110 | -58 | -81 | -65 |
| | Net change $N_c/\%$ | 1.00 | 0.98 | -0.37 | -1.80 | 5.54 | -2.76 | -0.26 | -0.35 | -0.57 |
| | Total change $T_c/\%$ | 103.92 | 103.96 | 94.21 | 133.30 | 161.99 | 119.78 | 99.97 | 103.64 | 93.56 |
| | Trend state index P_s | 0.01 | 0.01 | 0 | -0.01 | 0.03 | -0.02 | 0 | 0 | -0.01 |
| | Net rate of change $R_s/\%$ | 0.10 | 0.10 | -0.04 | -0.18 | 0.54 | -0.28 | -0.03 | -0.04 | -0.06 |
| 1990—1995 | Area variation/km ² | -37 | -621 | -397 | -359 | 39 | 135 | 4 526 | -1 253 | -2 030 |
| | Net change $N_c/\%$ | -0.10 | -21.55 | -4.52 | -10.45 | 13.64 | 3.48 | 20.55 | -5.48 | -18.04 |
| | Total change $T_c/\%$ | 102.87 | 122.07 | 107.75 | 145.11 | 175.17 | 139.78 | 130.16 | 121.72 | 88.90 |
| | Trend state index P_s | 0 | -0.18 | -0.04 | -0.07 | 0.08 | 0.02 | 0.16 | -0.04 | -0.20 |
| | Net rate of change $R_s/\%$ | -0.02 | -4.74 | -0.92 | -2.18 | 2.59 | 0.69 | 3.81 | -1.12 | -3.90 |
| 1995—2000 | Area variation/km ² | -133 | 549 | 508 | 496 | 5 | -279 | -4 769 | 2 615 | 1 016 |
| | Net change $N_c/\%$ | -0.37 | 24.28 | 6.05 | 16.12 | 1.54 | -6.95 | -17.96 | 12.09 | 11.01 |
| | Total change $T_c/\%$ | 104.15 | 161.96 | 118.31 | 170.46 | 172.62 | 140.48 | 110.07 | 131.79 | 108.75 |
| | Trend state index P_s | 0 | 0.15 | 0.05 | 0.09 | 0.01 | -0.05 | -0.16 | 0.09 | 0.10 |
| | Net rate of change $R_s/\%$ | -0.07 | 4.44 | 1.18 | 3.03 | 0.31 | -1.43 | -3.88 | 2.31 | 2.11 |
| 2000—2005 | Area variation/km ² | -1 131 | 125 | 129 | 57 | 718 | 454 | -400 | -399 | 447 |
| | Net change $N_c/\%$ | -3.16 | 4.45 | 1.45 | 1.60 | 217.58 | 12.16 | -1.84 | -1.65 | 4.37 |
| | Total change $T_c/\%$ | 3.84 | 7.86 | 2.39 | 2.32 | 221.21 | 20.24 | 4.61 | 3.43 | 7.24 |
| | Trend state index P_s | -0.82 | 0.57 | 0.61 | 0.69 | 0.98 | 0.60 | -0.40 | -0.48 | 0.60 |
| | Net rate of change $R_s/\%$ | -0.64 | 0.87 | 0.29 | 0.32 | 26.00 | 2.32 | -0.37 | -0.33 | 0.86 |
| 2005—2010 | Area variation/km ² | -138 | 2 | -4 | 12 | 117 | 2 | -2 | 66 | -55 |
| | Net change $N_c/\%$ | -0.40 | 0.07 | -0.04 | 0.33 | 11.16 | 0.05 | -0.01 | 0.28 | -0.51 |
| | Total change $T_c/\%$ | 0.48 | 0.14 | 0.13 | 0.39 | 11.16 | 0.76 | 0.40 | 0.49 | 1.39 |
| | Trend state index P_s | -0.82 | 0.50 | -0.33 | 0.86 | 1.00 | 0.06 | -0.02 | 0.56 | -0.37 |
| | Net rate of change $R_s/\%$ | -0.08 | 0.01 | -0.01 | 0.07 | 2.14 | 0.01 | 0 | 0.06 | -0.10 |
| 2010—2015 | Area variation/km ² | 72 | 2 | -33 | -18 | -13 | -20 | -283 | -368 | 662 |
| | Net change $N_c/\%$ | 0.21 | 0.07 | -0.37 | -0.49 | -1.12 | -0.48 | -1.32 | -1.54 | 6.23 |
| | Total change $T_c/\%$ | 1.95 | 2.66 | 0.99 | 2.09 | 20.17 | 6.30 | 2.61 | 2.30 | 9.92 |
| | Trend state index P_s | 0.11 | 0.03 | -0.37 | -0.24 | -0.06 | -0.08 | -0.51 | -0.67 | 0.63 |
| | Net rate of change $R_s/\%$ | 0.04 | 0.01 | -0.07 | -0.10 | -0.22 | -0.10 | -0.27 | -0.31 | 1.22 |
| 1980—2015 | Area variation/km ² | -1 012 | 85 | 170 | 125 | 881 | 182 | -986 | 580 | -25 |
| | Net change $N_c/\%$ | -2.84 | 2.98 | 1.93 | 3.57 | 325.09 | 4.56 | -4.46 | 2.53 | -0.22 |
| | Total change $T_c/\%$ | 6.30 | 11.95 | 5.55 | 7.92 | 332.47 | 29.78 | 10.87 | 13.72 | 29.67 |
| | Trend state index P_s | -0.45 | 0.25 | 0.35 | 0.45 | 0.98 | 0.15 | -0.41 | 0.18 | -0.01 |
| | Net rate of change $R_s/\%$ | -0.08 | 0.08 | 0.05 | 0.10 | 4.22 | 0.13 | -0.13 | 0.07 | -0.01 |

Tab. 2 Total trend index and composite net change rate of vegetation in the Hekouzhen-Longmen region of the middle reaches in the Yellow River

| Total index | 1980-1990 | 1990-1995 | 1995-2000 | 2000-2005 | 2005-2010 | 2010-2015 | 1980-2015 |
|-----------------------------------|-----------|-----------|-----------|-----------|-----------|-----------|-----------|
| Net change in total area $S_a/\%$ | 0.36 | 4.22 | 4.65 | 1.73 | 0.18 | 0.66 | 1.82 |
| Total change $S_s/\%$ | 51.45 | 57.19 | 58.44 | 2.67 | 0.31 | 1.61 | 6.44 |
| Total trend state index P_t | 0.01 | 0.07 | 0.08 | 0.65 | 0.57 | 0.41 | 0.28 |
| Total net rate of change $R_t/\%$ | 0.04 | 0.83 | 0.91 | 0.34 | 0.04 | 0.13 | 0.05 |

2.3 Impact of vegetation change on runoff

Vegetation change mainly affects the water cycle process of "precipitation-infiltration-evapo-transpiration-runoff" by changing the underlying conditions of the watershed^[3]. From the above quantitative analysis, it can be seen that the transformation direction of vegetation types in the river basin has changed significantly since 1980, especially the implementation of GGP in 1999, which makes the vegetation types in one-way transformation mainly from 2000 to 2016, is showing an imbalance. Besides, the terrain, geomorphology, and soil characteristics in the watershed are relatively stable, so the changes in the underlying surface of the watershed are mainly reflected by changes in vegetation. In order to quantify the impact of vegetation on runoff, this paper evaluates the runoff response to vegetation based on the Budyko elastic coefficient method^[27].

Tab. 3 shows the hydrometeorological characteristics in different periods in the Hekouzheng-Longmen region, as well as changes in underlying surface parameters n and their effects on runoff. It can be seen from Tab. 3 that the multi-year average runoff depth before the implementation of GGP (1980-1999) is 38.5 mm, but in the last 10 years after the implementation of GGP (2000-2010), although the precipitation shows an increasing trend, the runoff depth showed a sharp downward trend. The downward trend decreased from 2000 to 2005 by 7.2 mm compared to the previous period. From 2006 to 2010 it drops to 21.8 mm, a decrease of 43.4% compares to the previous GGP implementation. The underlying surface parameter n for the corresponding period is 2.05 before the GGP implementation, and increase to 2.51 after the implementation. Among them, the increase of n from 2000 to 2005 is 2.19, and the contribution rate of vegetation changes to the runoff caused by the implementation of GGP is 91.0%. From 2006 to 2010, n reaches 2.65, 29.3% higher than that before GGP implementation, and the contribution rate of vegetation to runoff is as high as 193.7%. The results are consistent with the response of the underlying surface parameter n . The increase of

vegetation corresponds to the decrease of runoff, indicating that the influence of vegetation on runoff is further strengthened. Therefore, vegetation change has become the main influencing factor of runoff decline in the last 10 years after the implementation of GGP. From 2011 to 2016, the underlying parameter n became 2.77, and precipitation continued to increase, which is increased by 57 mm compared to 2006-2010. The impact of vegetation on runoff decreased, and its contribution rate to runoff decreased to 38.6%. The results suggest that precipitation is the main factor affecting runoff, making runoff increase to 38.2 mm.

According to the above analysis, from 2000 to 2010 after the implementation of GGP, the underlying surface parameter n increases significantly, the contribution rate of vegetation to runoff increases, runoff decreases sharply, and vegetation changes become the main factor of runoff decline in the basin. With the continuous increase of precipitation in 2011-2016, the impact of vegetation on runoff decreases, and precipitation becomes the main factor for the increase of runoff in the basin, and the runoff depth shows an increasing trend.

In order to further analyze the relationship between vegetation changes and runoff in the Hekouzheng-Longmen region from 1980 to 2016, the Mann-Kendall test is used to detect the mutation points in the runoff time series (Fig. 3 (b)). It can be seen that the mutation point in the runoff time series is about 2004, which is the fifth year after the implementation of GGP, indicating that the effect of vegetation restoration is beginning to appear. The runoff depth decreased from 37.4 mm/a before the turning point to 26 mm/a with a decrease of 30.5% (Fig. 3 (a)). Similar to the findings of this paper, some studies have pointed out that the project of returning farmland to forests on the Loess Plateau has reduced regional water resource availability^[5,23]. However, although runoff depth shows a downward trend from 2004 to 2010 (-2.3 mm/a, $p < 0.01$), while from 2011 to 2016, runoff depth shows an increasing trend (4.6 mm/a, $p < 0.1$). Compared to the former turning point, the runoff coefficient (runoff depth/precipitation)

after the turning point has decreased (Fig. 3 (c)), indicating that the vegetation coverage of the watershed increases, changing the underlying surface conditions, resulting in the decrease of surface albedo and the increase of surface net radiation energy, which is consumed by vegetation through evaporation^[28]. When the amount of precipitation is not changed, higher evapotranspiration will lead to a decrease in the runoff coefficient, which may reduce the overall runoff capacity of the basin. Therefore, vegetation changes in this basin have significantly changed the hydrological process "precipitation-infiltration-evapotranspiration-runoff". However,

from 2011 to 2016, the vegetation coverage area in the Hekouzhen-Longmen region continues to increase. As precipitation continues to increase, the river basin's runoff capacity also continues to increase. The dryness index is an indicator of hydrothermal conditions, which can reflect the climatic characteristics of a region over a longer time scale^[29-30]. The dryness index in the Hekouzhen-Longmen region (Fig. 3 (d)) decreases from 2.22 (1980-2004) to 2.10 (2004-2016), especially with the increase of precipitation in 2011-2016, the dryness index reaches 1.93, is showing an overall "wetting" trend.

Tab. 3 Hydrometeorological factors and vegetation contribution to runoff during different periods in the Hekouzhen-Longmen region

| Period | Runoff | Precipitation | Potential evapotranspiration | Parameter n | Elasticity coefficient | Contribution amount | Contribution rate/% |
|-----------|--------|---------------|------------------------------|---------------|------------------------|---------------------|---------------------|
| 1980—1999 | 38.5 | 448.2 | 975 | 2.05 | -2.35 | | |
| 2000—2005 | 31.3 | 446.0 | 993 | 2.19 | -2.53 | -6.55 | 91.0 |
| 2006—2010 | 21.8 | 465.9 | 990 | 2.65 | -2.81 | -18.40 | 193.7 |
| 2011—2016 | 28.5 | 522.9 | 994 | 2.77 | -2.58 | -2.60 | -38.6 |
| 2000—2016 | 27.5 | 479.0 | 992 | 2.51 | -2.62 | -22.62 | 206.2 |

Note: The elastic coefficient refers to the elastic coefficient of the runoff to the vegetation parameter n , and the contribution amount refers to the contribution of vegetation to the runoff. Each period after 2000 is relative to the previous period.

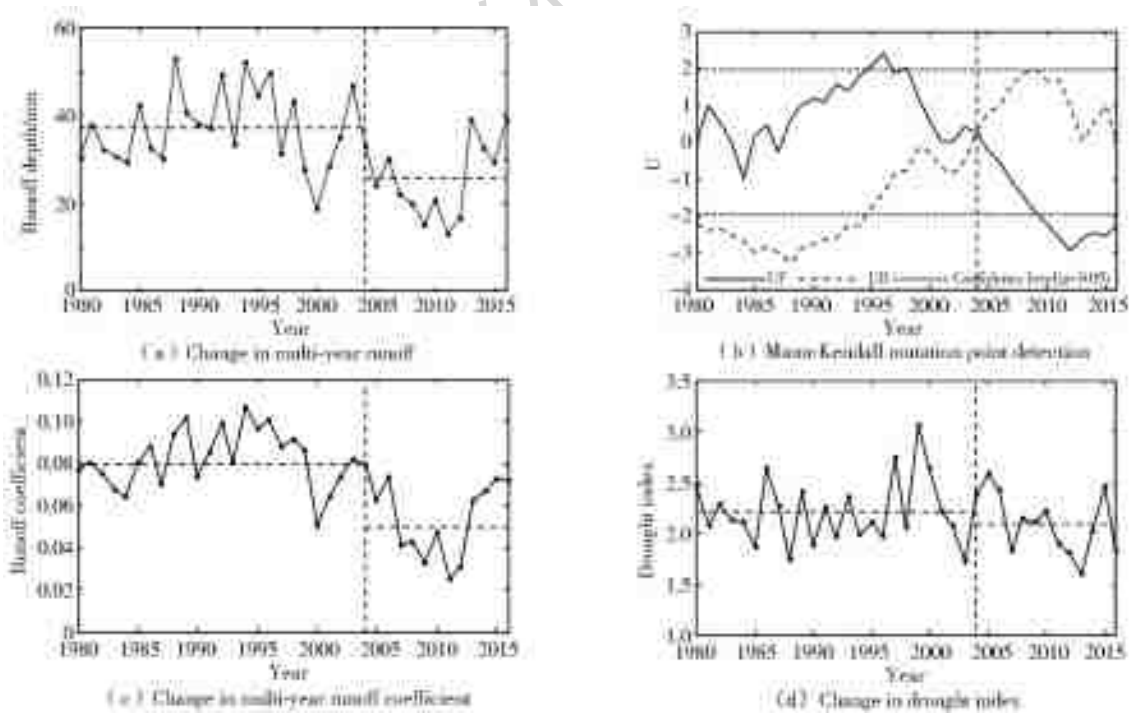


Fig. 3 Detection of runoff mutation point, runoff coefficient and drying index characteristics in the Hekouzhen-Longmen region of the middle reaches in the Yellow River

3 Conclusions

This paper analyzes the temporal and spatial

dynamics of vegetation in the Hekouzhen-Longmen region of the middle reaches in the Yellow River from 1980 to 2015 using vegetation type data, runoff

data, and meteorological data of seven periods using the elastic coefficient method based on Budyko framework to clarify the impact of vegetation on runoff. The results show that the implementation of GGP does not significantly change the spatial distribution pattern of each vegetation type in the Hekouzheng-Longmen region, but significantly alter the equilibrium state of each vegetation type, the change rate and direction of conversion between different types. The vegetation types change from the dynamic balance before GGP implementation, and the two-way conversion frequently changes to the imbalance after GGP implementation. The one-way conversion is mainly dominated by the conversion of cultivated land to other woodlands and high-coverage grasslands, which make the grassland area reduction trend be restrained. The rate of change in the later period slow down, and various types of vegetation tended to stabilize. Vegetation changes caused by the implementation of GGP in the Hekouzheng-Longmen region has a significant impact on runoff. Vegetation changes are the main reason for the runoff decline within 10 years after the implementation of the GGP project. Since then, precipitation has continued to increase and its "water reduction effect" has also eased. Strengthening the quantitative research on the vegetation change pattern in the Hekouzheng-Longmen region of the middle reaches in the Yellow River and its impact on runoff changes can provide a reference for the implementation of vegetation restoration projects and the development and utilization of water resources in the river basin.

References:

- [1] PIAO S, YIN G, TAN J, et al. Detection and attribution of vegetation greening trend in China over the last 30 years[J]. *Global Change Biology*, 2015, 21(4): 1601-1609. DOI:10.1111/gcb.12795.
- [2] FENG X, FU B, PIAO S, et al. Revegetation in China's Loess Plateau is approaching sustainable water resource limits[J]. *Nature Climate Change*, 2016, 6(11): 1019-1022. DOI:10.1038/nclimate3092.
- [3] JACKSON, R B. Trading Water for carbon with biological carbon sequestration[J]. *Science*, 2005, 310(5756): 1944-1947. DOI:10.1126/science.1119282.
- [4] PIAO S, CIAIS P, HUANG Y, et al. The impacts of climate change on water resources and agriculture in China [J]. *Nature*, 2010, 467(7311): 43-51. DOI:10.1038/nature09364.
- [5] SUN G, ZHOU G, ZHANG Z, et al. Potential water yield reduction due to forestation across China[J]. *Journal of Hydrology*, 2006, 328(3-4): 548-558. DOI:10.1016/j.jhydrol.2005.12.013.
- [6] LIANG W, YANG Q K. Land use change analysis in coarse sandy hilly catchments of Yellow River based on the remote sensing[J]. *Research of Soil and Water Conservation*, 2006, 13(5): 90-92. (in Chinese) DOI:10.3969/j.issn.1005-3409.2006.05.030.
- [7] LI G, LIANG W, YANG Q K. Analysis of land use pattern change in coarse sandy region of middle reaches of Yellow River[J]. *Science of Soil and Water Conservation*, 2009, 7(3): 52-58. (in Chinese) DOI:10.3969/j.issn.1672-3007.2009.03.010.
- [8] ZHOU D C, ZHAO S Q, ZHU C. Impacts of the sloping land conversion program on the land use/cover change in the Loess Plateau: A case study in Ansai County of Shaanxi Province, China [J]. *Journal of Natural Resources*, 2011, 26(11): 1866-1878. (in Chinese) DOI:10.11849/zrzyxb.2011.11.006.
- [9] LIU C M, LI Y Z, LIU X M, et al. Impact of vegetation change on water transformation in the middle Yellow River[J]. *Yellow River*, 2016, 38(10): 7-12. (in Chinese) DOI:10.3969/j.issn.1000-1379.2016.10.002.
- [10] LIU C M, ZHONG J X. The influence of forest cover upon annual runoff in the Loess Plateau of China[J]. *Acta Geographica Sinica*, 1978, 33(2): 112-127. (in Chinese) DOI:10.11821/xb197802003.
- [11] CAO S, CHEN L, YU X. Impact of China's Grain for Green Project on the landscape of vulnerable arid and semi-arid agricultural regions: a case study in northern Shaanxi Province [J]. *Journal of Applied Ecology*, 2009, 46(3): 536-543. DOI:10.1111/j.1365-2664.2008.01605.x.
- [12] CHEN Y. Balancing green and grain trade[J]. *Nature Geoscience*, 2015, 8(10): 739-741. DOI:10.1038/ngeo2544.
- [13] MCVICAR T R, LI L T, NIEL T G V, et al. Developing a decision support tool for China's re-vegetation program; Simulating regional impacts of afforestation on average annual streamflow in the Loess Plateau[J]. *Forest Ecology and Management*, 2007, 251(1): 65-81. DOI:10.1016/j.foreco.2007.06.025.
- [14] YANG S T, ZHOU X, LIU X Y, et al. Impacts of land use on vegetation coverage in the rich and coarse sediment area of Yellow River basin[J]. *Acta Geographica*

- Sinica, 2014, 75(1): 31-41. (in Chinese) DOI: 10. 11821/dlxb201401003.
- [15] LI Y Z, LIU C M, LIU X M, et al. Impact of the Grain for Green Project on the land use/cover change in the Middle Yellow River[J]. Journal of Natural Resources, 2016, 31 (12): 2005-2020. (in Chinese) DOI: CNKI; SUN; ZRZX. 0. 2016-12-004.
- [16] LI Y, LIU C, ZHANG D, et al. Reduced runoff due to anthropogenic intervention in the Loess Plateau, China [J]. Water, 2016, 8 (458): 1-16. DOI: 10. 3390/w8100458.
- [17] LIANG K, LIU C, LIU X, et al. Impacts of climate variability and human activity on streamflow decrease in a sediment concentrated region in the Middle Yellow River[J]. Stochastic Environmental Research & Risk Assessment, 2013, 27 (7): 1741-1749. DOI: 10. 1007/s00477-013-0713-2.
- [18] FATHIAN F, DEHGHAN Z, BAZRKAR M H, et al. Trends in hydrologic and climatic variables affected by four variations of Mann-Kendall approach in Urmia Lake basin, Iran [J]. Hydrological Sciences Journal, 2016, 61 (5): 892-904. DOI: 10. 1080/02626667. 2014. 932911.
- [19] ALLEN R G, PEREIRA L S, RAES D, et al. Crop evapotranspiration-Guidelines for computing crop water requirements-FAO Irrigation and drainage paper 56 [M]. FAO, 1998. DOI: 10. 1007/978-3-319-05699-9_6.
- [20] LIU X, LIU W, XIA J. Comparison of the streamflow sensitivity to aridity index between the Danjiangkou Reservoir basin and Miyun Reservoir basin, China [J]. Theoretical and Applied Climatology, 2013, 111 (3-4): 683-691. DOI: 10. 1007/s00704-012-0701-3.
- [21] MCCUEN R H. A sensitivity and error analysis of procedures used for estimating evaporation[J]. Journal of the American Water Resources Association, 1974, 10(3): 486-497. DOI: 10. 1111/j. 1752-1688. 1974. tb00590. x.
- [22] CONG Z, SHAHID M, ZHANG D, et al. Attribution of runoff change in the alpine basin; a case study of the Heihe Upstream basin, China [J]. Hydrological Sciences Journal, 2017, 62 (6): 1013-1028. DOI: 10. 1080/02626667. 2017. 1283043.
- [23] LIANG W, BAI D, WANG F, et al. Quantifying the impacts of climate change and ecological restoration on streamflow changes based on a Budyko hydrological model in China's Loess Plateau [J]. Water Resources Research, 2015, 51 (8): 6500-6519. DOI: 10. 1002/2014wr016589.
- [24] YANG D W, ZHANG S L, XU X Y. Attribution analysis for runoff decline in Yellow River basin during past fifty years based on Budyko hypothesis [J]. Science China Technological Sciences, 2015, 45: 1024 - 1034. (in Chinese) DOI: 10. 1360/N092015-00013.
- [25] RODERICK M L, FARQUHAR G D. A simple framework for relating variations in runoff to variations in climatic conditions and catchment properties [J]. Water Resources Research, 2011, 47 (12). DOI: 10. 1029/2010WR009826.
- [26] ZHANG S, YANG H, YANG D, et al. Quantifying the effect of vegetation change on the regional water balance within the Budyko Framework [J]. Geophysical Research Letters, 2015, 43 (3): 1140-1148. DOI: 10. 1002/2015GL066952.
- [27] LIU X M, LUO Y Z, ZHANG D, et al. Recent changes in pan-evaporation dynamics in China [J]. Geophysical Research Letters, 2011, 38 (38): 142-154. DOI: 10. 1029/2011gl047929.
- [28] MYKLEBY P M, LENTERS J D, Cutrell G J, et al. Energy and water balance response of a vegetated wetland to herbicide treatment of invasive phragmites australis [J]. Journal of Hydrology, 2016, 539: 290-303. DOI: 10. 1016/j. jhydrol. 2016. 05. 015.
- [29] LIU X, ZHANG D, LUO Y, et al. Spatial and temporal changes in aridity index in northwest China; 1960 to 2010 [J]. Theoretical and applied climatology. 2013, 112 (1-2): 307-316. DOI: 10. 1007/s00704-012-0734-7.
- [30] LI Y, FENG A, LIU W, et al. Variation of aridity index and the role of climate variables in the southwest China [J]. Water, 2017, 9 (10): 743. DOI: 10. 3390/w9100743.